

Purcell factor and superradiance in Si-patterned waveguides

A. Pitanti,^{1,3,*} P. Bettotti,¹ D. Sarchi,² and L. Pavesi¹

¹Nanoscience Laboratory, Department of Physics, University of Trento, via Sommarive 14, Povo (TN), Italy

²BEC Center, Department of Physics, University of Trento, via Sommarive 14, Povo (TN), Italy

³Current address: NEST, Scuola Normale Superiore and Istituto di Nanoscienze-CNR, Piazza San Silvestro 12, Pisa, Italy

*Corresponding author: pitanti@science.unitn.it

Received April 19, 2010; revised August 11, 2010; accepted August 11, 2010;

posted September 17, 2010 (Doc. ID 127121); published October 8, 2010

Numerical modeling of slotted photonic crystal Si waveguides is reported. Employing multiple slots in a single waveguide, we obtained large Purcell enhancements for a large ensemble of emitters coupled with the same optical mode. This allows observation of peculiar physical phenomena, such as anisotropic bandgap superradiance. © 2010 Optical Society of America

OCIS codes: 130.5296, 270.6630.

While a large photon density of states (DOS) can be realized in dielectric microcavities [1] and photonic crystals [2–4], its spatial localization is strongly limited by the electromagnetic field shape. It can be seen that the local DOS (LDOS) scales with the square of the field amplitude, being null in proximity of field nodes [5]. This fact is important when spontaneous emission (SE) rate enhancements due to large DOS (Purcell effect) are investigated. The Purcell enhancement is proportional to the LDOS, and thus it is subjected to the same spatial limitations. This is particularly important when a large ensemble of emitters is considered, since it has to be placed very close to a field antinode to experience noteworthy enhancements. For this reason, the Purcell effect mainly has been exploited to create single photon sources, in which a *single* emitter is placed as close as possible to a field antinode [6]. This limits the possibility of exploiting collective phenomena due to a large ensemble of emitters.

In this Letter, we propose a photonic crystal waveguide (PhCw) geometry where large DOS enhancements can be obtained in specific large areas. The geometry of the proposed PhCw is depicted in Fig. 1. A periodic sequence of slots is dug into a silicon rib waveguide. The slots are filled with Er-doped SiO₂ (Er is the emitter considered). The geometrical parameters of the PhCw have been optimized for maximum enhancement where Er³⁺ emission is localized, i.e., at 1.535 μm [7]. Geometrical parameters are reported in the inset to Fig. 1.

A first modeling of the system is carried out with a two-dimensional (2D) calculation ($h \rightarrow \infty$). Figure 1(b) shows the photonic bands of the Bloch modes for TE polarization, obtained with a plane-wave code [8]. Usually the modes are localized in the high-index Si dielectric, with field nodes within the slots. A different situation is found for the third photonic band, whose Bloch modes are strongly confined within the slots. This is a consequence of the electric field discontinuity at the interfaces between the high- and low-index materials; this situation is similar to what is found in the so-called slot waveguides [9]. Figure 1(b) also shows the group-velocity dispersion associated to this third band. A large reduction in group velocity is observed for the frequencies close to the band edge.

To calculate the Purcell factor (F_P), we consider the ratio between the analytical Bloch-mode Green's function of the proposed PhCw and the Green's tensor of a homogeneous media as in [10]:

$$F_P(\omega, \vec{r}) = \frac{3\pi c^3 \Lambda}{\omega^2 \sqrt{\epsilon} v_g} |u_{\vec{k}(\vec{r})}|^2,$$

where ϵ is the dielectric constant, ω is the angular frequency, Λ is the PhCw period, and v_g (c) is the group (light) velocity. $u_{\vec{k}(\vec{r})}$ is the optical field within the photonic crystal fundamental cell. It is worth noting that $F_P \propto v_g^{-1}$, which shows the potential to obtain large Purcell factors for slow group-velocity modes at the band-edge frequencies. The F_P values for the third photonic band of Fig. 1, calculated in the center of the fundamental cell [labeled with coordinate (0,0)] for a PhCw of infinite length, are shown in Fig. 2(a). Also in Fig. 2(a), we show an F_P map at the reciprocal lattice point $[0,0,0.5] 2\pi/\Lambda$. F_P up to 60 can be obtained for an optical mode which is strongly localized within the slots and has a negligible component in the Si dielectric. As expected, being the LDOS (and thus F_P) inversely proportional to v_g , F_P progressively decreases moving away from the band edge.

A second modeling of the system is performed to consider finite size effects, assuming a finite PhCw length. We used an open-source finite-difference time-domain

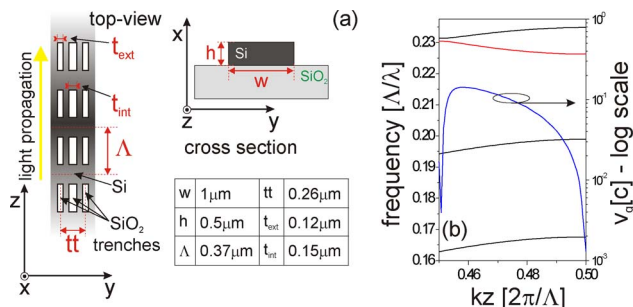


Fig. 1. (Color online) (a) Sketch of the PhCw. Periodic SiO₂ slots are patterned in a Si rib waveguide along the light propagation direction (z). Waveguide dimensions are reported in the table. (b) TE photonic bands and third band group velocity for the PhCw waveguide (PWE method [8]).

software package [11] and evaluated F_P by the method proposed in [12]. The PhCw studied is composed of 15 periods ($15 - \Lambda$). Figure 2(b) reports the results. As expected, while F_P maintains large values in the center of the PhCw, it gradually decreases toward the edges. In this case, it is also interesting to evaluate the ratio of the emitted photons that are coupled into the Bloch modes (coupling constant β) for an emitter placed in the center of the structure of Fig. 2(b). Disregarding the nonradiative recombination rate [13], a β value of 0.95 has been obtained for an emission that is spectrally tuned with the band-edge frequency, which is comparable with the best theoretical results obtained in the literature [14,15]. When a realistic finite height is considered, as reported in the table of Fig. 1(a), a three-dimensional (3D) F_P map can be obtained. We show some F_P isosurface maps in Fig. 2(c) for an infinitely long PhCw with the geometrical parameters of Fig. 1(a). Note that a minimum $F_P \geq 18$ is achieved for the whole slot volume for the third photonic band of our PhCw. If we assume that the slots are filled with an Er concentration of $1 \times 10^{20} \text{ cm}^{-3}$, it will result in approximately 4×10^6 ions subjected to a F_P that is equal to or larger than 18. This is significantly more than what can be achieved from the very same material when the photonic crystal waveguide designed in [14] is used. In

this case, only 7.85×10^2 ions are subjected to the same enhancement.

These findings suggest the possibility of coupling a large number of emitters with the same slow-light Bloch mode, which is intriguing for achieving novel physical regimes, like Dicke superradiance (SR) [16–18]. SR is a collective effect that is due to the coupling of closely spaced emitters to the same radiation field and includes the term superradiance, because the photoluminescence (PL) intensity of SR emission is proportional to the square of the number of emitters N . In contrast, in the uncorrelated case, a linear proportionality to N holds. In addition, more complicated models predict a N^3 proportionality for the SR effect in anisotropic photonic bandgaps [19], such as the one studied here. In the small-volume approximation, where the active volume is smaller than the cube of the radiation wavelength, an SR regime can be achieved if [17]

$$\tau_t \ll \tau_{\text{SR}} = \frac{2\pi n d^2 \omega v_g}{\hbar L} \ll \tau_{\text{SE}}, \quad (1)$$

where τ_t represents the photon transit time across the slot of length L ($\tau_t = L/v_g$) and τ_{SE} is the radiative lifetime of the emitter. n is the emitter concentration, while d is their dipole matrix element. τ_{SR} is the inverse of the SR recombination rate: because it is dependent on v_g , Purcell enhancements or slow-light effects directly determine its value. The inequality in the left-hand part of Eq. (1) prevents the occurrence of stimulated emission effects, while the right-hand one guarantees that no emitters recombine independently. Our proposed PhCw structure fulfills the small-volume approximation, since the slot volume $V_{\text{cell}} \sim 4 \times 10^{-14} \text{ cm}^3 \ll \lambda^3 \sim 3.6 \times 10^{-12} \text{ cm}^3$.

Figure 3(a) reports a 2D analysis of Eq. (1), considering only a single cell in an infinite PhCw, at different frequencies and for various Er^{3+} concentrations [20]. While τ_{SE} is always several orders of magnitude longer than the other characteristic times, the SR condition [Eq. (1)] is well verified for all doping levels only far from the band edge. Conversely, at the band edge, only the lower doping concentration fulfills the SR condition, due to the significant v_g reduction.

Let us now consider a sequence of slots filled with Er ions. Independent SR emissions from different slots are expected. It is of interest to find out when these emissions can produce coherent SR pulses instead. To this end we consider a finite $15 - \Lambda$ structure, as shown in Fig. 2(b). Uniformly distributed Er ions in the slots and the band-edge frequency tuned at $\lambda = 1535 \text{ nm}$ (Er emission wavelength) are considered. Each PhCw period is labeled with an increasing/decreasing integer number starting from the central, zeroth cell at $(0, 0) \mu\text{m}$ in Fig. 2(b). The LDOS decrease toward the PhCw edges is observed as a lengthening of τ_{SR} for emitters placed in external slots [symbols in Fig. 3(b)]. Different situations with respect to the SR condition of Eq. (1) are observed, depending on the Er concentration. Let us fix as initial condition a fully excited Er population where both spontaneous SR emission and stimulated emission can occur. The most probable SR emission in the system comes at first from the zeroth cell, where τ_{SR} is the shortest. Then, if the SR pulse propagates

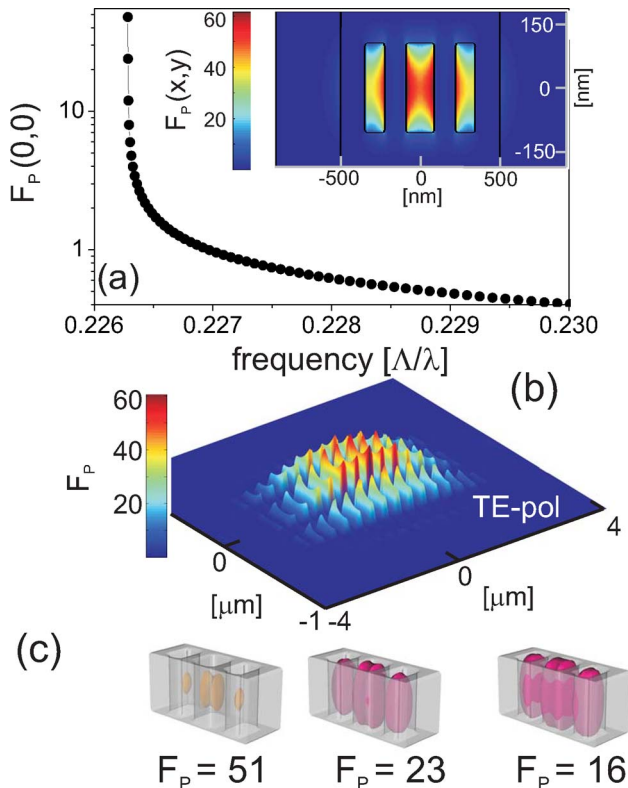


Fig. 2. (Color online) (a) F_P calculated for the third photonic band of the 2D, infinite length waveguide. F_P map in the y - z plane at band-edge frequency is reported in the inset. (b) F_P intensity map in the y - z plane calculated for the same band in the 2D, finite length (composed of 15 periods) waveguide, at band-edge frequency. (c) F_P isosurfaces in the fundamental cell ($0.5 \mu\text{m} \times 1 \mu\text{m} \times 0.37 \mu\text{m}$) calculated for the 3D, infinite length waveguide reported in Fig. 1(a) at band-edge frequency, shown within the dielectric structure.

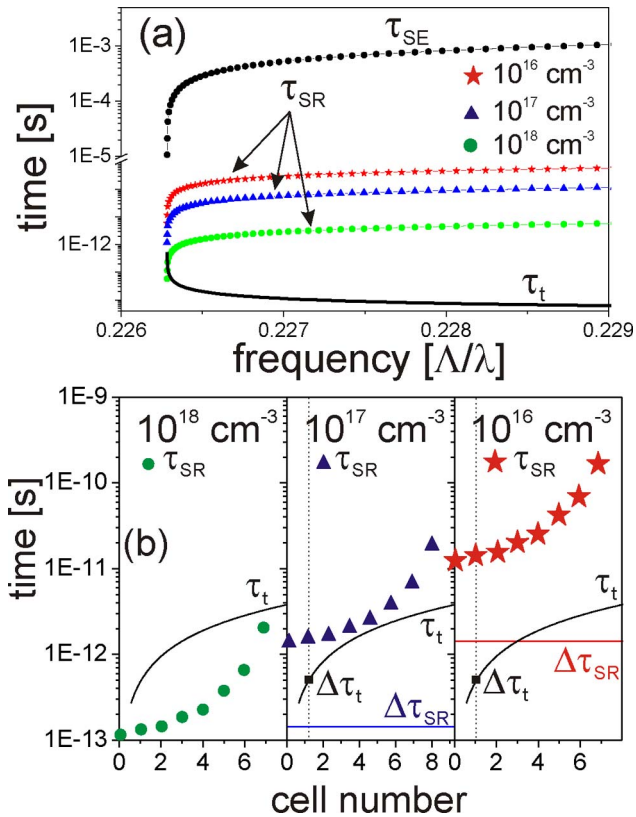


Fig. 3. (Color online) (a) SR condition in a single cell of an infinite PhCw for different doping concentration. (b) Comparison of τ_{SR} (•, ▲, ★) and τ_t (solid curve) in every cell of differently Er-doped PhCws. The SR ($\Delta\tau_{SR}$ —solid curve) and transit ($\Delta\tau_t$ —black squares) time differences between cell 0 and cell 1 are reported for completeness.

to the neighboring cells (1 and -1) in a time, $\Delta\tau_t$ [black square in Fig. 3(b)], that is shorter than the difference of τ_{SR} between cell 0 and cell 1 [$\Delta\tau_{SR} = \tau_{SR,1} - \tau_{SR,0}$, solid curves in Fig. 3(b)], the SR pulse will trigger stimulated emissions from the excited Er ions from cell 1. This has two consequences: (i) the Er ions relax to the ground state preventing further superradiant emission, and (ii) the SR pulse emitted from cell 0 is amplified. As a consequence, in *cascade*, the SR pulse emitted by the central slot will be amplified coherently by traveling through the waveguide. Conversely, if $\Delta\tau_t$ is shorter than $\Delta\tau_{SR}$, cells ± 1 will emit their own SR pulses that are noncoherent with the one emitted by cell 0. Looking at the results in Figs. 3(a) and 3(b), we note that for an Er concentration of $1 \times 10^{18} \text{ cm}^{-3}$, no SR pulse is expected. For $n = 1 \times 10^{17} \text{ cm}^{-3}$, the SR condition of Eq. (1) is fulfilled for every cell in the structure; however, the SR pulse emitted in the cell 0 will reach the cell ± 1 after its own SR emission ($\Delta\tau_t > \Delta\tau_{SR}$), with the generation of incoherent light. Finally, for a concentration of $1 \times 10^{16} \text{ cm}^{-3}$, the SR condition is fulfilled and the transit time $\Delta\tau_t$ is short enough to grant stimulated emission in the neighboring cells. An SR pulse thus will be generated and amplified in the structure. Even though rough approximations have been used here and no

structural imperfections were taken into account, the band-edge SR model of [19] applied here demonstrates that the emission from 500 emitters in the zeroth cell ($n = 1 \times 10^{16} \text{ cm}^{-3}$) equals the standard PL emission of 125×10^6 independent emitters, with the additional properties of coherence and spatial directionality. In conclusion, we have shown the potential to control the electromagnetic field to realize large DOS only in regions where active emitters are present. Beyond the interest of this finding for investigation of multiple-emitter fundamental physics, the proposed PhCw could be of interest for the development of compact Si-based light sources.

Funding from Provincia Autonoma di Trento (project GOPSI) and from the European Commission (EC) (project FP7-ICT HELIOS) is acknowledged.

References and Notes

1. J. M. Gérard, B. Sermage, B. Gayral, B. Legrand, E. Costard, and V. Thierry-Mieg, Phys. Rev. Lett. **81**, 1110 (1998).
2. P. Lodahl, A. F. van Drie, I. S. Nikolaev, A. Irman, K. Overgaag, D. Vanmaekelbergh, and W. L. Vos, Nature **430**, 654 (2004).
3. A. Kress, F. Hofbauer, N. Reinelt, M. Kaniber, H. J. Krenner, R. Meyer, G. Böhm, and J. J. Finley, Phys. Rev. B **71**, 241304 (R) (2005).
4. D. Englund, D. Fattal, E. Waks, G. Solomon, B. Zhang, T. Nakaoka, Y. Arakawa, Y. Yamamoto, and J. Vuckovic, Phys. Rev. Lett. **95**, 013904 (2005).
5. R. Sprik, B. A. van Tiggelen, and A. Lagendijk, Europhys. Lett. **35**, 265 (1996).
6. T. Lund-Hansen, S. Stobbe, B. Julsgaard, H. Thyrrstrup, T. Süner, M. Kamp, A. Forchel, and P. Lodahl, Phys. Rev. Lett. **101**, 113903 (2008).
7. P. C. Becker, N. A. Olson, and J. R. Simpson, *Erbium Doped Fiber Amplifier: Fundamental and Technology* (Academic, 1999).
8. S. G. Johnson and J. D. Joannopoulos, Opt. Express **8**, 173 (2001).
9. V. R. Almeida, Q. Xu, C. A. Barrios, and M. Lipson, Opt. Lett. **29**, 1209 (2004).
10. S. Hughes, Opt. Lett. **29**, 2659 (2004).
11. A. F. Oskooi, D. Roundy, M. Ibanescu, P. Bermel, J. D. Joannopoulos, and S. G. Johnson, Comput. Phys. Commun. **181**, 687 (2010).
12. A. J. Ward and J. B. Pendry, Phys. Rev. B **58**, 7252 (1998).
13. This can be a reasonable assumption for a concentration of Er^{3+} ions below the clusterization limit or for low-temperature emission.
14. V. S. C. Manga Rao and S. Hughes, Phys. Rev. B **75**, 205 (2007).
15. Y. C. Jun, R. M. Briggs, H. A. Atwater, and M. L. Brongersma, Opt. Express **17**, 7479 (2009).
16. R. H. Dicke, Phys. Rev. **93**, 99 (1954).
17. A. V. Andreev, V. I. Emel'yanov, and Yu. A. Il'inskii, Sov. Phys. Usp. **23**, 493 (1980).
18. M. Scheibner, T. Schmidt, L. Worschech, A. Forchel, G. Bacher, T. Passow, and D. Hommel, Nature Phys. **3**, 106 (2007).
19. S. John and T. Quang, Phys. Rev. Lett. **74**, 3419 (1995).
20. The optical constant of Er-doped SiO_2 material has been taken from the literature [7].